

Dynamics of wet flue gas desulphurization in spray absorber

M. M. Petrovic^a, V. D. Stevanovic^b, S. Jankovic^d and S. Milivojevic^c

^a *University of Belgrade, Faculty of Mechanical Engineering, Kraljice Marije 16, Belgrade, Serbia, mlpetrovic@mas.bg.ac.rs,*

^b *University of Belgrade, Faculty of Mechanical Engineering, Kraljice Marije 16, Belgrade, Serbia, vstevanovic@mas.bg.ac.rs,*

^c *University of Belgrade, Faculty of Mechanical Engineering, Kraljice Marije 16, Belgrade, Serbia, smilivojevic@mas.bg.ac.rs,*

^d *University of Belgrade, Faculty of Mechanical Engineering, Kraljice Marije 16, Belgrade, Serbia, stevan.jankovic@live.com*

Abstract:

A concise one dimensional thermal-hydraulic two-fluid model is presented for the numerical prediction of sulphur dioxide absorption from the flue gas onto drops of the water-limestone slurry in the vertical spray tower absorber. The model is based on mass, momentum and energy balance equations for each phase separately, i.e. downward falling droplets of water-limestone slurry and upward flowing flue gas. The sulphur dioxide content in the flue gas is predicted by a balance equation of the sulphur dioxide mass fraction in the flue gas. Interface transfer processes between the flue gas and the droplets are determined by closure laws. The obtained steady-state balance equations are transformed in a form suitable for a direct application of the numerical integration method for the system of ordinary differential equations. The developed thermal-hydraulic model is validated by comparing numerical results with available measured data at the large utility absorber. The presented results clearly show the dynamics of flue gas and droplets thermal-hydraulic processes and their influence on the absorption process.

Keywords:

Wet flue gas, Desulphurization, Absorption, Evaporation, Two-phase flow.

1. Introduction

The common flue-gas desulphurization (FGD) technology at large utility boilers is absorption of sulphur oxide (SO₂) in droplets of aqueous suspension of finely ground limestone in the spray tower absorber [1]. The efficiency of SO₂ absorption in the spray tower absorber strongly depends on the thermal and hydraulic interactions between the droplets and flue gas in counter-current flow. Although the wet limestone FGD is the mature technology, there is still a need for the development of prediction methods that can support the optimal design of such equipment that results in reduced investment costs and high reliability of operation and efficiency of SO₂ removal from the flue gas. Previous investigations of the SO₂ absorption in water-limestone slurry in wet scrubbers are extensive and only a few representative ones are reported in this paper. Nygaard et al. [2] have performed full-scale measurements of SO₂ gas phase concentrations and slurry compositions in a wet flue gas desulphurisation spray absorber at the large 620 MWe utility plant. They showed the efficiency of FGD and the spatial distribution of the process parameters in the spray tower absorber. A three dimensional prediction of slurry droplets and flue gas counter-current flow with SO₂ absorption was done by Marocco and Inzoli [3] with the commercial Computational Fluid Dynamics (CFD) code for the tower absorber conditions of a pilot plant. A CFD simulation of the FGD in tower absorber was also performed by Arif et al. [4] with a special attention to water consumption requirements. A one-dimensional model of SO₂ absorber was developed by Zhu et al. [5]. The influences of operating parameters on the absorption height were analysed. The modelling of SO₂ absorption rate in the slurry droplets was analysed by Saboni and Alexandrova [6]. Dou at

al. [7] investigated a desulphurization method based on the electrostatic spraying absorber and showed the relation between the sulphur-dioxide removal rate and the applied voltage at various slurry flow rates. A CFD simulation of sulphur-dioxide with enhancement factor analysis was performed by Gao et al. [8]. They also showed that increasing of pH value leads to exponential rise of enhancement factor of the absorption rate.

In the present paper a concise one-dimensional thermal-hydraulic two-fluid model is presented for the numerical prediction of sulphur dioxide absorption from the flue gas in drops of the water-limestone slurry in the spray tower absorber. The model is based on mass, momentum and energy balance equations for each phase separately, i.e. downward falling droplets of water-limestone slurry and upward flowing flue gas. The sulphur dioxide content in the flue gas is predicted by a balance equation of the sulphur dioxide mass fraction in the flue gas. Interface transfer processes between the flue gas and the droplets are determined by closure laws. The obtained numerical results are compared with available measured data from the large tower absorber in a utility power plant [2].

2. Thermal-hydraulic two-fluid model of spray tower absorber

The developed two-fluid model is based on mass, momentum and energy balance equations for each phase separately. One phase is water-limestone slurry and the other is flue gas. The water-limestone slurry flows downwards in form of dispersed droplets and flue gas flows upwards in form continuous phase. Transfer processes at the interfaces of the flue gas and the droplets, as well as between the fluid streams and the walls are calculated by the closure laws. The balance equations have the following form for transient one-dimensional flow conditions. The sulphur-dioxide and water contents in the flue gas are predicted by corresponding mass fraction balance equations.

2.1 Balance equations

Mass Balance

$$\frac{\partial(\alpha_k \rho_k)}{\partial t} + \nabla \cdot (\alpha_k \rho_k \bar{u}_k) = (-1)^{k+1} \Gamma_a + (-1)^k \Gamma_e \quad (1)$$

Momentum Balance

$$\begin{aligned} \frac{\partial(\alpha_k \rho_k \bar{u}_k)}{\partial t} + \nabla \cdot (\alpha_k \rho_k \bar{u}_k \bar{u}_k) = & -\alpha_k \nabla p + (-1)^{k+1} \alpha_k \rho_k \bar{g} + (-1)^{k+1} \tau_{12} a_{12} + \\ & + (-1)^k \tau_{kw} a_{kw} + (-1)^k \Gamma_e \bar{u}_1 + (-1)^{k+1} \Gamma_a \bar{u}_2 \end{aligned} \quad (2)$$

Energy Balance

$$\frac{\partial(\alpha_k \rho_k h_k)}{\partial t} + \nabla \cdot (\alpha_k \rho_k h_k \bar{u}_k) = (-1)^k \Gamma_e h_{H_2O}'' + (-1)^{k+1} \Gamma_a h_{SO_2} + (-1)^{k+1} \dot{q}_{21} + (2-k) \dot{m}_k h_k \quad (3)$$

Mass fraction of sulphur-dioxide in the flue gas

$$\frac{\partial(\alpha_2 \rho_2 g_{SO_2})}{\partial t} + \nabla \cdot (\alpha_2 \rho_2 \vec{u}_2 g_{SO_2}) = -\Gamma_a \quad (4)$$

Mass fraction of water vapour in the flue gas

$$\frac{\partial(\alpha_2 \rho_2 g_{H_2O})}{\partial t} + \nabla \cdot (\alpha_2 \rho_2 \vec{u}_2 g_{H_2O}) = \Gamma_e \quad (5)$$

The right hand side of Eqs. (1-3) represents mass, momentum and energy source terms. Index k=1 denotes liquid phase and k=2 denotes gas phase. The additional equation is volume fraction balance

$$\sum_{k=1}^2 \alpha_k = 1 \quad (6)$$

2.2 Closure laws

Mass, momentum and energy transfer at liquid and gas interface, as well as at fluid-wall interface are calculated by the closure laws given in Table 1. Interface processes such as evaporation, absorption, friction between droplets and flue gas, friction between fluid and wall and heat transfer from flue gas to droplets are taken into account in developed multi-fluid model. The rate of evaporation (T1-1) is determined by the gas side mass transfer coefficient between water and flue gas, water vapour partial pressure difference between the interface and the bulk of the mixture and molar mass of water. Gas side mass transfer coefficient is calculated according to modified Ranz-Marshall equation and it depends on thermal-hydraulic parameters and binary diffusion coefficient of water in air. The rate of sulphur-dioxide absorption (T1-2) is calculated using global mass transfer coefficient, sulphur-dioxide partial pressure difference between the flue gas and the interface, and molar mass of sulphur-dioxide. The global mass transfer coefficient involves both gas and liquid side mass transfer coefficients and Henry constant for sulphur-dioxide. Partial pressure of sulphur-dioxide at the interface is determined by sulphur-dioxide concentration in droplets. Thermal-hydraulic parameters and binary liquid diffusion coefficient of sulphur-dioxide in liquid is calculated by evaporation terms analogy (T1-1). The interfacial shear stress and drag coefficient are determined in (T1-3). The wall shear stress is given in (T1-4). Convective heat transfer between phases is presented by the source term (T1-5).

2.3 Numerical solution

The steady-state conditions in the tower absorber were assumed. The first terms on the l.h.s. of Eqs. (1-5) are equal to zero for steady-state conditions. Equations (1-5) were transformed in the form with spatial derivatives of the dependent parameters on the l.h.s. of equations, which enables direct numerical solution by the Runge-Kutta method for the initial spatial conditions prescribed at the top exit cross section of the absorber. The prescribed initial values of the dependent parameters are void fractions, velocities and enthalpies of the slurry droplets and the flue gas, as well as the water vapour and SO₂ concentrations in the flue gas.

Table 1. Closure laws

Interface process		
Evaporation		
$j_e = k_{H_2O,g} (p_{H_2O,i} - p_{H_2O,\infty}) M_{H_2O}$	$\Gamma_e = j_e a_{12}$	$p_{H_2O,\infty} = \frac{g_{H_2O} p_{fg} R_{H_2O}}{R_{fg}}$
$k_{H_2O,g} = \frac{D_{H_2O,g}}{d_d RT_2} (2 + 0.69 \text{Re}_r^{0.5} S_c^{0.33})$ [9]	$p_{H_2O,i} = p_{sat}(T_d)$	$\text{Re}_r = \frac{\rho_2 u_2 - u_1 d_d}{\mu_2}$
$D_{H_2O,g} = \frac{435.7 \cdot 10^{-4} T_2^{1.5} \left[\frac{1}{M_{H_2O}} + \frac{1}{M_g} \right]^{0.5}}{p_{dg} \left(v_{H_2O}^{\frac{1}{3}} + v_g^{\frac{1}{3}} \right)^2}$ [10]	$S_c = \frac{\rho_2}{\mu_2 D_{H_2O,g}}$	(T1-1)
Absorption		
$j_a = k_{SO_2} (p_{SO_2,\infty} - p_{SO_2,i}) M_{SO_2}$	$\Gamma_a = j_a a_{12}$	$p_{SO_2,i} = H_{SO_2} C_{SO_2,i}$
$\ln(H_{SO_2}) = \frac{A}{T_d} + B \ln(T_d) + CT_d + D$ [11]	$p_{SO_2,\infty} = \frac{g_{SO_2} p_{fg} R_{SO_2}}{R_{fg}}$	$k_l = 10 \frac{D_{SO_2,l}}{d_d}$ [12]
$k_g = \frac{D_{SO_2,g}}{d_d RT_d} (2 + 0.69 \text{Re}_r^{0.5} S_c^{0.33})$ [9]	$k_{SO_2} = \frac{1}{\frac{1}{k_g} + \frac{H_{SO_2}}{Ek_l}}$	$Sc = \frac{\mu_2}{\rho_2 D_{SO_2,g}}$
$D_{SO_2,g} = \frac{435.7 \cdot 10^{-4} T_2^{1.5} \left[\frac{1}{M_{SO_2}} + \frac{1}{M_g} \right]^{0.5}}{p_{dg} \left(v_{SO_2}^{\frac{1}{3}} + v_g^{\frac{1}{3}} \right)^2}$ [10]	$\text{Re}_r = \frac{\rho_2 u_2 - u_1 d_d}{\mu_2}$	(T1-2)
Droplets-flue gas friction		
$f_{12} = \frac{24}{\text{Re}_r} (1 + 0.15 \cdot \text{Re}_r^{0.687}) + \frac{0.42}{1 + 4.25 \cdot 10^{-4} \cdot \text{Re}_r^{-1.16}}$ [13]	$\tau_{12} = \frac{1}{8} f_{12} \rho_2 u_2 - u_1 \cdot (u_2 - u_1)$	$a_{12} = \frac{6\alpha_d}{d_d}$
	$\text{Re}_r = \frac{\rho_2 u_2 - u_1 d_d}{\mu_2}$	(T1-3)
Fluid-wall friction		
$f_{kw} = \frac{F}{\text{Re}_r^n}$	$\tau_{kw} = f_{kw} \frac{\rho_k u_k u_k}{2}$	
For turbulent flow, $F=0.079$, $n=0.25$	$\text{Re}_r = \frac{\rho_k u_k D_h}{\mu_k}$	
For turbulent flow, $F=16$, $n=1$		(T1-4)
Flue gas-droplets heat transfer		
$Nu_{21} = \frac{h_{21} d_d}{k_2} = 2 + 0.6 \text{Re}_r^{0.5} \text{Pr}_2^{0.33}$ [14]	$\dot{q}_{21} = h_{21} (T_2 - T_1) a_{12}$	$\text{Pr}_2 = \frac{\mu_2}{\rho_2 a_2}$
	$\text{Re}_r = \frac{\rho_2 u_2 - u_1 d_d}{\mu_2}$	(T1-5)

3. Results and Discussion

The developed two-fluid model of counter-current upward flue gas and downward slurry droplets flow with SO₂ absorption is applied to the prediction of measured conditions in the spray tower absorber at Unit 5 of the 620 MWe Thermal Power Plant Asnæs in Denmark, as reported in [2]. The tower absorber dimensions and locations of five spray levels for water-limestone slurry introduction are presented in Fig. 1. The operating parameters of the tower absorber during performed measurements are presented in Table 2. The SO₂ concentrations were measured by gas analyzer in samples of flue gas that were extracted from the absorber inner volume. Direct measurements of SO₂ concentration in the absorber were not possible due to the impact of slurry drops [2]. Figure 2 shows the flue gas and slurry droplets change along the spray tower absorber. The zero height is positioned at the level of flue gas inlet. As presented, the flue gas temperature rapidly drops approximately along the first 8 m from the inlet, from the inlet value of 137 °C to the 60.4 °C, which is only about 1 °C higher than the droplets temperature at that level. This rapid decrease is caused by the much larger thermal capacity of the droplets stream than the flue gas stream and the large interfacial area between droplets and flue gas. The flue gas-droplets interfacial area concentration is calculated as $6\alpha_d/d_d$, as presented in Table 1 by equations under (T1-3). For the droplets volume fraction of 1 %, i.e. $\alpha_d=0.01$ and droplets diameter 2 mm, the interfacial area concentration reaches even 30 m² per m³ of flue gas-droplets two-phase mixture. Along the remaining flow path, above the level of 8 m from the flue gas inlet, the temperature of the flue gas is only slightly higher than the droplets temperature. The flue gas-droplets temperature difference constantly decreases towards the spray tower exit and it practically diminishes at the flue gas outlet from the tower.

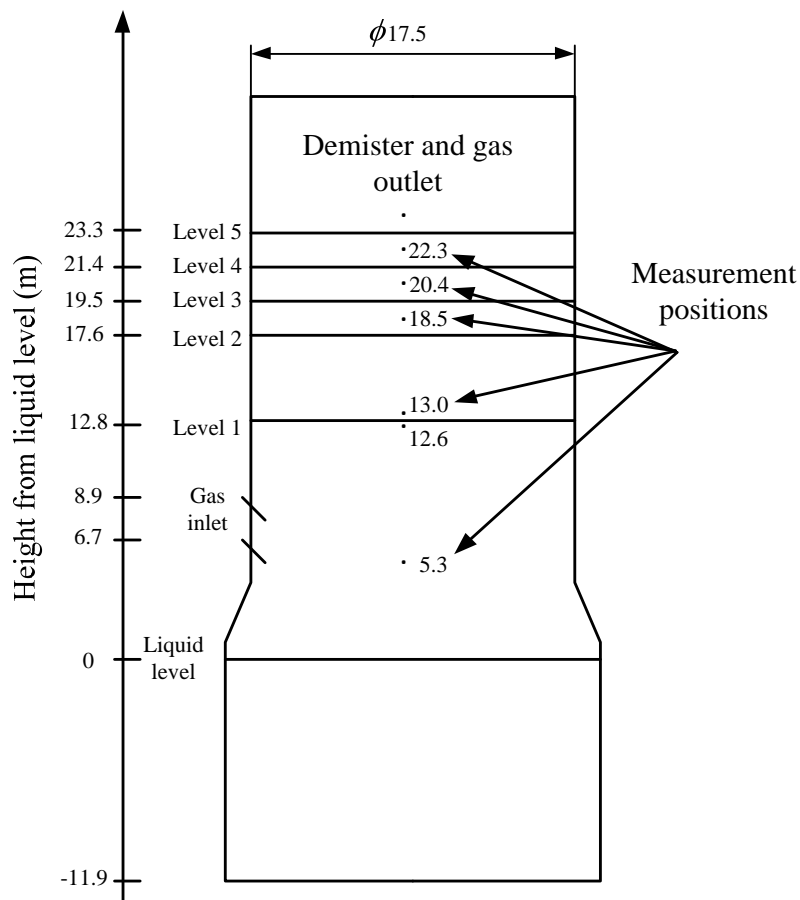


Fig. 1 Layout of the spray tower absorber in 620 MWe Thermal Power Plant Asnæs [2].

Table 2. Design data of spray tower absorber

FGD installation at Asnæs power plant	
Column diameter	17.5 m
Nozzle levels	5
Number of nozzles per level	184
Absorber height from liquid level	23.3 m
Gas flow rate	$2 \cdot 10^6 \text{ Nm}^3/\text{h}$
Liquid flow rate per nozzle	779 l/min
Liquid flow rate per nozzle level	$8600 \text{ Nm}^3/\text{h}$
Operation pressure	1 atm
Height from the centre of the gas inlet to nozzle level 1	6.1 m
Height from the centre of the gas inlet to nozzle level 2	10.9 m
Height from the centre of the gas inlet to nozzle level 3	12.8 m
Height from the centre of the gas inlet to nozzle level 4	14.7 m
Height from the centre of the gas inlet to nozzle level 5	16.6 m
Approximate slurry volume of holding tank	3925 m^3
Inlet flue gas temperature	125-150 °C (137 °C ¹)
Inlet sulphur-dioxide concentration	375-425 ppv (400 ppmv ¹)
Droplet diameter	2-3mm (2 mm ¹)

Note: ¹Operational parameters assumed in the calculation.

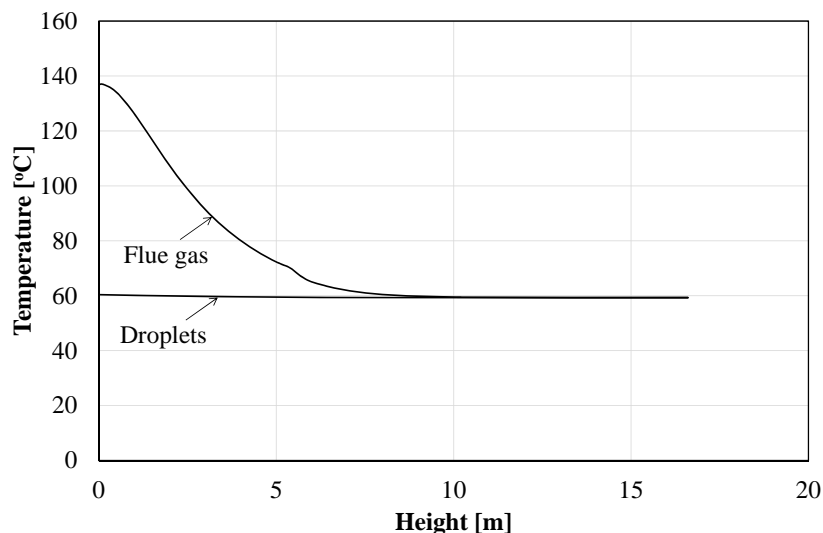


Fig. 2. Flue gas and slurry droplets temperature change along the tower absorber starting from the cross section of the flue gas inlet.

Droplets volume fraction in the two-phase mixture with the flue gas is presented in Fig. 3. The zero level corresponds to the flue gas inlet, while the droplets nozzles at the highest top level, indicated as level 5 in Fig. 1, are positioned at 16.6 m from the flue gas inlet. At the locations of droplets inlet nozzles the droplets volume fraction increases, while downstream it decreases because of droplets acceleration due to gravity. Five peaks of droplets volume fraction in Fig. 3 corresponds to droplets inlet at the location of five nozzles. The highest droplets volume fraction is about 1.2% just below the lowest droplets nozzles at the level 1 at the height of 6.1 m (Fig. 1) and it slightly decreases to 1.1% at the flue gas inlet level at 0 m.

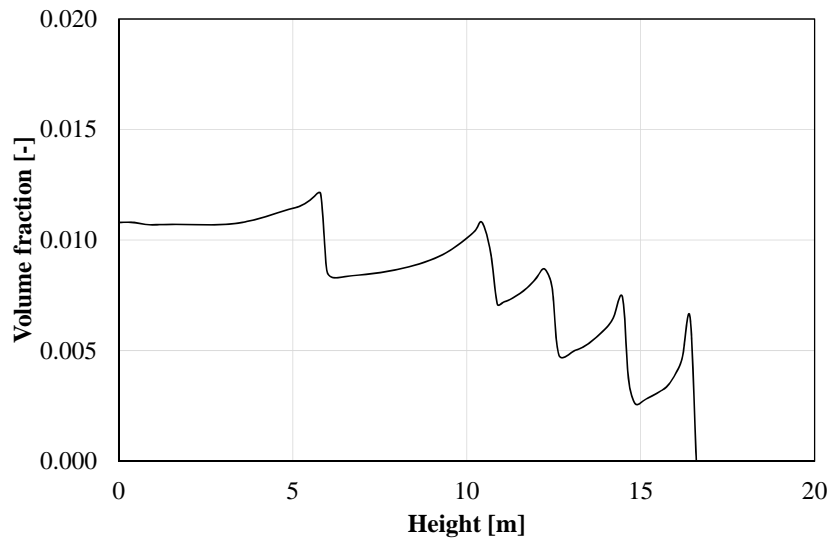


Fig. 3. Droplets volume fraction.

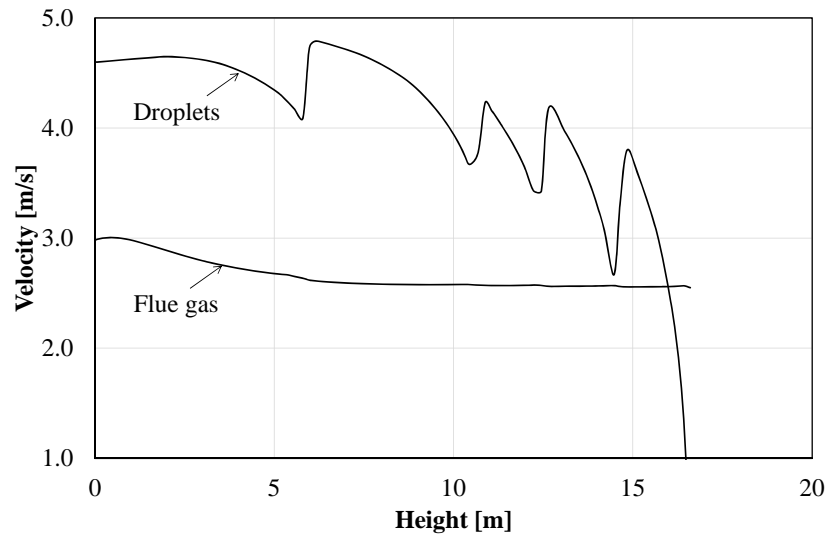


Fig. 4. Flue gas and droplets velocities.

Figure 4 shows that the flue gas velocity change along the spray tower height is smooth, while droplets velocity rapidly increases below inlet nozzles due to gravity and decreases in zones of nozzles injections due to their lower injection velocity (the lower injection velocity decelerate the falling droplets rain). The flue gas velocity slightly decreases along the first several meters at the entrance due to the gas cooling and gas specific volume decrease.

The pressure change along the spray tower is shown in Fig. 5. The pressure of two-phase mixture decreases constantly along the spray tower from the flue gas inlet at the bottom to the top exit level. The two-phase mixture density and corresponding hydrostatic pressure change have the largest impact on the pressure decrease along the absorber spray tower.

Figure 6 shows the stepwise increase of the droplets mass flow rate from the top to the bottom of the spray tower at the locations of droplets injections by the nozzles. The mass flow rate of injected droplets is 2627.8 kg/s and this amount is the same at each nozzles level. The mass flow rate of droplets in the falling spray equals the amount of the injected droplets above approximately 9 m,

since the flue gas above 9 m is almost equal to the droplets temperature (as presented in Fig. 2) and practically there is no evaporation within this upper volume of the absorber. The evaporation takes place from the flue gas inlet at 0 m and up to approximately 9 m, where the temperature difference between the flue gas and droplets is substantial. The difference of mass flow rates of injected water droplets and droplets falling into the pool at the absorber bottom is approximately 34 kg/s, which is less than 0.3% of injected droplets mass flow rate. But, during the long term operation, this mass of evaporated water reaches considerable amount of approximately 120 t/h. Therefore, the reduction of flue gas temperature at the inlet of the absorber and the corresponding reduction of the droplets evaporation are important for the saving of water.

Measured and calculated SO₂ concentrations along the spray tower are presented in Fig. 7. As presented, the SO₂ concentration decrease is the most intensive in the central region of the tower, above the first level of droplets nozzles at 6.1 m and below the fourth nozzles level at 14.7 m. Below 6 m the absorption rate is lower because the droplets are saturated with sulphur, while in the tower top part close to the flue gas outlet, the SO₂ concentration in the flue gas is low and the mass transfer at the fresh injected droplets is low.

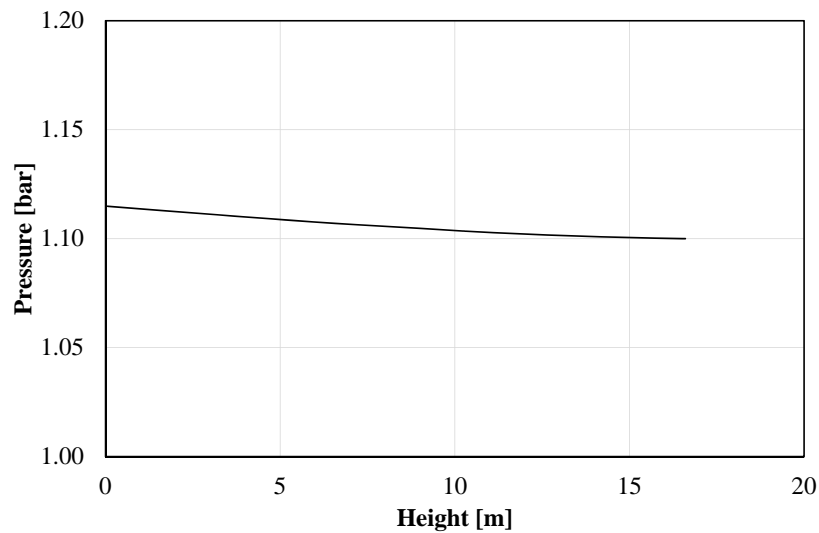


Fig. 5. Pressure change along the spray tower.

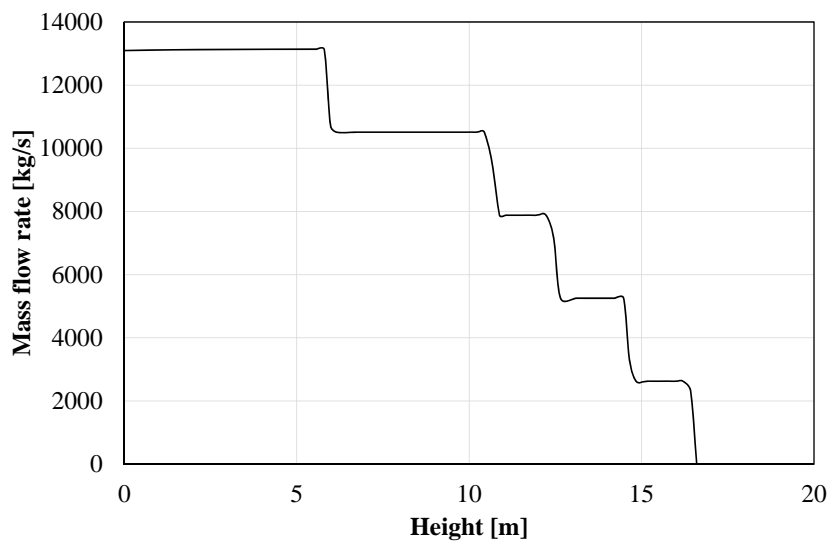


Fig. 6. Droplets mass flow rate in the spray tower.

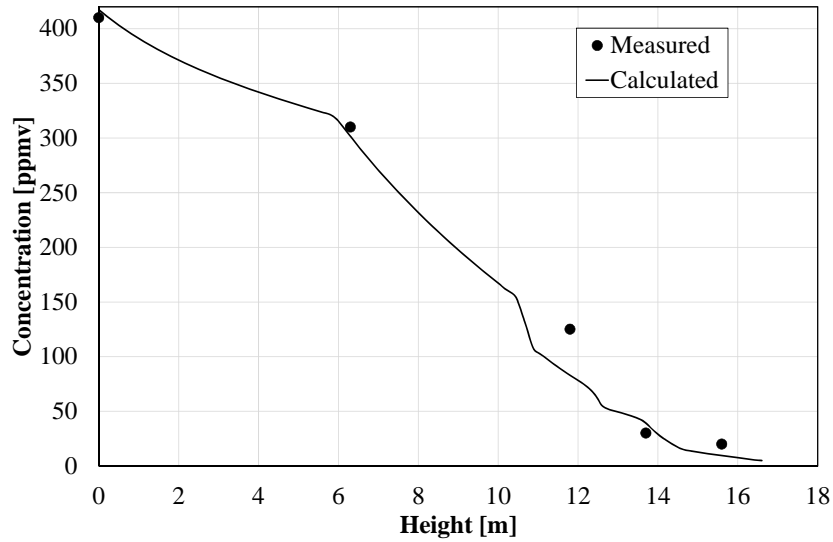


Fig. 7. Comparison of measured and calculated SO₂ concentration.

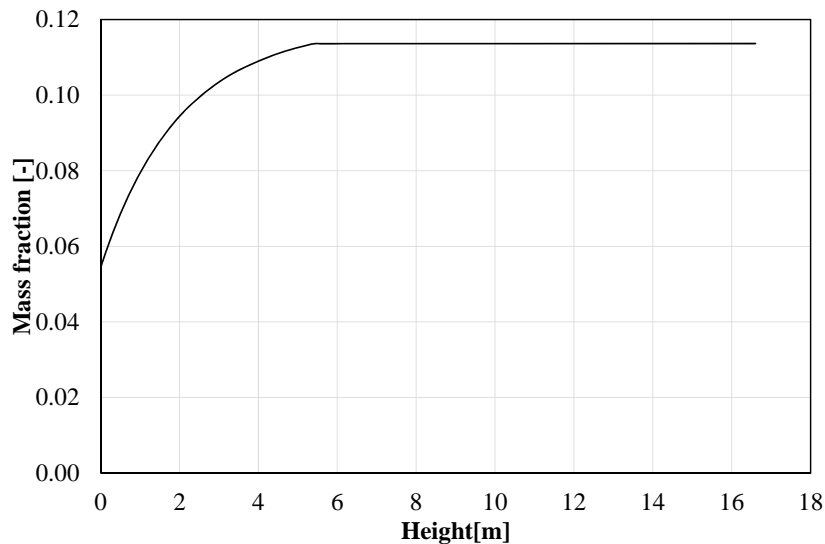


Fig.8. Water vapour mass fraction in the mixture with flue gas.

Figure 8 shows that the flue gas is saturated with the water vapour in the area close to the flue gas inlet. Approximately after 5 m from the flue gas inlet the flue gas is saturated with water vapour.

4. Conclusions

The model for the prediction of counter-current flue gas and droplets flow and SO₂ removal from the flue gas in the spray tower absorber is developed. The model is solved numerically for the conditions of the large utility plant tower absorber. The obtained results are compared with the available measured data and a good agreement is obtained. It is shown that the large interfacial area leads to rapid thermal equilibrium between the flue gas and slurry droplets. The SO₂ absorption is intensive almost along the whole height of the tower absorber. Droplets injections through nozzles at several levels have a strong influence on the thermal-hydraulic conditions in the tower absorber. In addition, the model predicts water evaporation in the spray tower, which is important for the calculation of water losses in flue gas desulphurization process. The influence of the flue gas and droplets temperature difference on the droplets evaporation is shown and the possibility for the water savings by the reduction of the flue gas temperature at the absorber inlet is indicated. The developed model is a support to the spray tower design.

Nomenclature

a	interfacial area concentration, 1/m, thermal diffusivity, m ² /s
C	concentration, mol/ m ³
d_p	average droplet size, m
D	diffusion coefficient, m ² /s
D_h	hydraulic diameter of absorber, m
E	enhancement factor, -
f	friction coefficient, -
g	mass fraction, gravity, m/s ²
h	heat transfer coefficient, W/(m ² K), specific enthalpy, J/kg
j_a	rate of absorption, kg/(m ² s)
j_e	rate of evaporation, kg/(m ² s)
h	heat transfer coefficient, W/(m ² K), specific enthalpy, J/kg
k	thermal conductivity, W/(m K)
M	molecular mass, g/mol
\dot{m}	mass flow rate, kg/s
Pr	Prandtl number, -
p	pressure, Pa
\dot{q}	volumetric heat rate, W/ m ³
Sc	Schmidt number, -
T	temperature, K
\vec{u}	velocity vector, m/s

Greek symbols

α	volume fraction, -
Γ^a	rate of absorption, kg/(m ³ s)
Γ^e	rate of evaporation, kg/(m ³ s)
μ	dynamic viscosity, kg/(m s)
v	molecule volume, cm ³ /mol
ρ	density, kg/m ³

Subscripts and superscripts

d	droplet
fg	flue gas
g	air
H_2O	water
i	interface
k	phase indicator (k=1-liquid, k=2-flue gas)
r	relative
sat	saturation
w	wall

References

- [1] Best available techniques for large combustion plants, European Commission 2006-Available at: <http://eippcb.jrc.ec.europa.eu/reference/BREF/lcp_bref_0706.pdf>.[accessed 29.02.2016].
- [2] Nygaard H.G., Kiilb S., Johnssonb J.E., Jensen J.N., Hansen J., Foghc F., Dam-Johansenb K., Full-scale measurements of SO₂ gas phase concentrations and slurry compositions in a wet flue gas desulphurisation spray absorber. *Fuel* 2004;83:1151–1164.
- [3] Marocco L., Inzoli F., Multiphase Euler–Lagrange CFD simulation applied to Wet Flue Gas Desulphurisation technology. *International Journal of Multiphase Flow* 2009;35:185–194.
- [4] Arif A., Stephen C., Branken D., Everson R., Neomagus H., Piketh S., Modeling Wet Flue Gas Desulfurization, Conference of the National Association for Clean Air (NACA 2015), South Africa, 2015-Available at:<https://www.researchgate.net/profile/David_Branken/publication/282672302_Modeling_Wet_Flue_Gas_Desulfurization/links/56180b5808ae6d17308487bc.pdf>.[accessed 29.02.2016]
- [5] Zhu J.,Ye S., Bai J., Wu Z., Liu Z.,Yang Y., A concise algorithm for calculating absorption height in spray tower for wet limestone–gypsum flue gas desulfurization. *Fuel Processing Technology* 2015;129:15–23.
- [6] Saboni A., Alexandrova S., Sulfur dioxide absorption and desorption by water drops. *Chemical Engineering Journal* 2001;84:577–580.
- [7] Dou B. L., Byun Y. C., Hwang J., Flue gas desulfurization with an electrostatic spraying absorber. *Energy & fuel* 2008; 22:1041-1045.
- [8] Gao X., Huo W., Luo Z. Y., Cen K. F., CFD simulation with enhancement factor of sulphur dioxide absorption in spray scrubber. *Journal of Zhejiang University SCIENCE A* 2008; 9(11): 1601-1613.
- [9] Rowe P. N., Claxton K. T., Lewis J. B., Heat and mass transfer from a single sphere in an extensive flowing fluid. *Trans. Inst. Chem.* 1965;43.
- [10] Holman J. P., *Heat Transfer*, Ninth ed. New York: McGraw-Hill; 1990.
- [11] Maurer G., On the solubility of volatile weak electrolytes in aqueous solutions. *ACS Symp* 1980: Ser.133;139-172.
- [12] Perry R. H., Green, Don W., *Chemical Engineers Handbook*, seventh ed. USA: McGraw-Hill; 1998.
- [13] Clift R., Grace J. R., Weber M. E., *Bubbles, drops, and particles*. New York: Academic press; 1978.
- [14] Ranz W. E., Marshall, W. R., Evaporation from drops, I and II. *Chem. Eng. Program*1952; 48/3-48/4;22,141-146,173-180.